Room temperature hardness of carbides-strengthened cast alloys in relation with their carbon content and the aging temperature. Part I: Case of nickel alloys

Patrice Berthod

Room temperature hardness of carbides-strengthened cast alloys in relation with their carbon content and the aging temperature. Part I: Case of nickel alloys

Patrice BERTHOD
Laboratoire de Chimie du Solide Minéral (CNRS UMR 7555)
Faculté des Sciences et Techniques, Université Henri Poincaré Nancy 1, Nancy-Université,
Boulevard des Aiguillettes, BP 239, F-54506 VANDOEUVRE LES NANCY, FRANCE
patrice.berthod@centraliens-lille.org

Post-print version of the article: Materials Science and Technology (2009) 25(5) 657-662.
DOI 10.1179/174328408X339242

Keywords: Nickel alloy, Chromium carbides, Aging treatment, Vickers indentation, Hardness, Micro-hardness

Abstract.
The addition of hard particles in a ductile alloy may lead to a substantial increase in its hardness and in the difficulty to machine it. This work aims to specify the role of chromium carbides in the hardness of cast nickel alloys. A Ni-30 wt.%Cr alloy and six {0 to 2 wt.%C}–containing alloys based on the first one, were elaborated by foundry. Their microstructures after aging at 1,000, 1,100 and 1,200°C were described, and the room temperature Vickers hardness of all alloys for the three aging treatments was measured. Hardness increases with carbon content following a curve which is almost parabolic, while it increases more linearly versus the volume fraction of carbides. Hardness is generally lowered by choosing higher aging temperature. The evolution of hardness was compared with a law of mixture based on the hardness and the volume fractions of the matrix and of the carbides.

1. Introduction

Nickel base alloys are extensively used for many applications. Chromium–rich versions are met in several domains, for example in dentistry for frameworks in prostheses[1,2] or in

aeronautics and power generation for turbine blades[3,4], where chromium allows a good resistance against aqueous corrosion or high temperature oxidation.

The hardness of {Ni, Cr}–based carbon–containing alloys are to be taken into account to predict the easiness of machining pieces from such alloys. Curiously, hardness studies, or hardness measurements in more general studies, are not very numerous concerning structural cast alloys based on such compositions. Indeed, such attention is predominantly focused on coatings (e.g. Ni-WC, Ni-Cr_3C_2) deposited or formed by several techniques (thermal spray, plasma jet, plasma carburization, induction or laser cladding, …), with a special attention to wear resistance only[5-8].

The aim of this work is to specify the hardness of ternary Ni-Cr-C alloys, which can be considered as the bases of numerous chromia–forming superalloys strengthened by carbides. The Cr content was chosen to be 30 wt.% Cr, which is an usual content ensuring the resistance against oxidation and corrosion at high temperature for long times. The studied carbon content varies from 0 to 2.0 wt.%, which covers what is usually present in such superalloys.

2. Experimental

2.1 Preparation of the samples

The targeted carbon contents in the 30 wt.%Cr–containing alloys studied here, which are respectively called Ni00, Ni02, Ni04, Ni08, Ni12, Ni16 and Ni20, are respectively 0, 0.2, 0.4, 0.8, 1.2, 1.6 and 2 wt.%C. All alloys were elaborated by foundry from pure elements (nickel and chromium: Alfa Aesar, purity higher than 99.9 wt.%; carbon: graphite). Each alloy (about 100g) was obtained by melting these elements together, in inert atmosphere (300 mbar of Argon U), using a CELES high frequency induction furnace. Fusion and solidification took place in a water–cooled copper crucible.

In each ingot three parallelepipedic samples (about 10 mm × 10 mm × 3 mm) were cut using a Buehler Isomet 5000 precision saw. They were polished with paper from 240 to 1,200 grit. The three samples from each alloy were thereafter exposed for 50 hours to 1,000°C, 1,100°C or 1,200°C in a tubular resistive furnace (atmosphere: air), followed by cooling to room temperature with a rate of about 10 K min^{-1}. After these high temperature exposures each sample was cut in two equal parts and embedded in a resin + hardener mixture (Escil CY230

+ HY956). The mounted samples were then polished with paper from 240 to 1,200 grit and polishing was finished using a 1µm Al_2O_3–paste.

2.2 Metallography

The polished samples were etched using Groesbeck solution (4g of $KMnO_4$ and 4g of NaOH in 100 mL of distilled water), during 60 seconds at room temperature. Microstructure observations were done using an optical microscope (Olympus AH2) equipped with a digital camera (Olympus DP11) for taking numerical micrographs. Carbides were identified using a Cameca SX100 microprobe for pinpoint analysis by Wavelength Dispersion Spectrometry (WDS).

In order to estimate the volume fractions of carbides, three micrographs were taken in areas which were randomly chosen near the centre of each sample, with a magnification leading to areas of about 0.023 mm². This allowed having both a representative view of the microstructure and a sufficient precision for the image analysis measurements. The latter were performed of the three optical micrographs realized for each {alloy, aging temperature} couple, using the Adobe Photoshop CS software.

2.3 Thermodynamic calculations

In order to contribute to the knowledge of the natures of the phases existing at the three aging temperatures, and also at lower temperatures, calculations were performed using the Thermo-Calc software[9] and a database containing the descriptions of the Ni-Cr, Ni-C, Cr-C and Ni-Cr-C systems[10-12].

2.4 Hardness measurements

Hardness was measured for all of the seven nickel–based alloys in their three aged states. Two types of hardness were considered. First, three Vickers hardness measurements were performed using a Testwell Wolpert apparatus with a load of 30 kg, with calculation of the average value and the standard deviation. In addition, five Vickers micro-hardness measurements (with a load of 8g) were performed in matrix (apparatus: Reichert model D32), also with calculation of the average value and of the standard deviation. In the rare cases

when this was possible, the hardness of the coarsest carbides was also measured (Reichert model D32 with a load of 32g).

3. Results

3.1 Microstructures of the alloys

The matrix of the binary Ni-30wt.%Cr is face centred cubic at room temperature as well as at all higher temperatures, according to the binary Ni-Cr diagram for this Cr content. The matrixes of all the carbon–containing alloys are also face centred cubic. These ternary alloys also contain a carbide phase, the identification of which was possible by WDS measurements only for the three carbon–richest alloys; in these alloys carbides are all of the M_7C_3 type. Thermo-Calc calculations showed that carbides are effectively M_7C_3 for temperatures between about 1,300°C and at least 1,000°C (and even less than 500°C for the three C–richest alloys). At lower temperatures, carbides must be $M_{23}C_6$ according to the equilibria calculated by Thermo-Calc. However, because of the cooling rate which was not sufficiently low, the time spent by the alloy at the temperatures for which transformations may occur, was obviously too short to allow the M_7C_3 -> $M_{23}C_6$ change. This explains why carbides are still M_7C_3 at room temperature, as shown by WDS or by the brown colour of carbides after Groesbeck etching.

Carbides are of course more present when the carbon content in the alloy is high (Fig. 1). When the carbon content begins increasing, the dendritic structure of the matrix becomes more visible. Thereafter, dendrites of matrix progressively disappear and they do not exist anymore when the carbon content is higher than 1.2 wt.%. In the Ni20 alloy, several primary carbides, formed prior to the eutectic solidification, can be seen.

After Groesbeck etching, the contrast between the pale matrix and the carbides coloured in brown is sufficient to perform image analysis. The results (average value for three micrographs ± standard deviation) are presented in Fig. 2. It was verified that they are generally consistent with the fractions calculated with Thermo-Calc (after conversion of the calculated mass fractions in volume fractions). The graph clearly shows the increase in surface fraction when the carbon content increases in the alloy. The slope becomes slightly lower for the highest carbon contents, although the dependence could be considered almost linear (about 12 surface percent of carbide per weight percent of carbon). In addition, the surface fraction of carbides tends to be slightly lower when the aging temperature is higher.

3.2 Vickers macro-hardness measurements

Vickers hardness measurements, with a load of 30 kg, were performed three times near the centre of each sample, with calculations of the average value and of the standard deviation (which was taken as uncertainty). All the measures are plotted in Fig. 3.

The first graph (Fig. 3a) presents the variation of hardness versus the carbon content in the alloy, with three curves corresponding to the three temperatures of aging. One can see the increase in hardness when the carbon content increases, without linearity since the curves are parabolic. Hardness rapidly increases when carbon begins to be added to the binary alloy, but the addition of the same quantity of carbon to an alloy already containing carbon, leads to a smaller increase in hardness. This is true for each of the three aging temperatures. But one can also notice that, for the same carbon content, the hardness of the carbon-containing alloys aged at 1,200°C is significantly lower than the hardness of the same alloys but aged at 1,000°C only. The curve corresponding to the alloys aged at 1,100°C is merged with the curve for 1,200°C when the carbon content is low. In contrast, for the alloys with high carbon contents the curve for 1,100°C becomes merged with the curve for 1,000°C. It can also be noticed that the hardness difference between an alloy aged at 1,200°C and the same alloy aged at 1,000°C is zero for the binary alloy, increases up to almost 50 Hv_{30kg} for the medium carbon contents and decreases down to around 25 Hv_{30kg} for the carbon–richest alloys.

The second graph (Fig. 3b) presents the evolution of hardness versus the carbide surface fraction as estimated by image analysis. This mode of representation takes into account the tendency of less pronounced increase in carbide fraction with the enrichment in carbon, seen above with the curves in Fig. 2. This allows noticing an almost linear variation of hardness with the carbides quantity. The rate of increase in hardness when the carbides fraction increases, is around 5 to 6 Hv_{30kg} per volume percent of carbide.

3.3 Vickers micro-hardness measurements

Five Vickers hardness measurements were performed with a load of 8g in the matrix of each alloy aged at the three aging temperatures. The hardness of matrix, which is fcc in all cases, may depend on its chemical composition.

The chromium content in matrix was measured by WDS microanalysis, with sometimes dispersed results in the carbides–richest alloys. The latter phenomenon is due to interactions with subjacent carbides, and this is favoured when the carbide fraction becomes very high. On the contrary chromium was correctly analyzed in the matrix of the alloys with less carbide, and the results were consistent with the values of chromium content in matrix predicted by thermodynamic calculations. Carbon contents cannot be quantified by micro-analysis because of the too low atomic mass of this element and its too low content in matrix. Therefore, it must be deduced from Thermo-Calc calculations. The possibility to obtain a unique value for the chromium content in matrix (validated by WDS microanalysis for the alloys with low carbide fractions) and also to have a predicted value for the carbon content in matrix, led to prefer using the Cr and C contents in matrix calculated by Thermo-Calc, for all alloys and all aging temperatures. The evolution of the micro-hardness in matrix is plotted in Fig. 4 versus the chromium content (Fig. 4a) and versus the carbon content (Fig. 4b). There is no clear dependence of the hardness of matrix on its chemical composition, and the results vary around the average value of 200 Hv_{8g}.

Unfortunately, it was almost never possible to perform, in sufficiently good conditions, micro-hardness measurements on the carbides in these alloys. However this was nevertheless tried on an especially coarse carbide seen in the cross section of the Ni20 alloy aged at 1,000°C. Its Vickers micro-hardness measurement, performed with a load of 32g to obtain a sufficient pyramid size, led to a value of 1,192 Hv_{32g}.

4. Discussion

The addition of 30 wt.%Cr did not lead to a noticeable change from the hardness of pure nickel. In contrast the enrichment in carbon promotes a significant increase in hardness. Indeed, the addition of 1 wt.% C doubles the Hv_{30kg} number while the increase still goes on (but is not so high) for new additions of carbon up to a total content of 2 wt.%C. High values of hardness were thus obtained but they are not so high as martensitic annealed steels or as a hard-facing 0.45C-2B-10Cr nickel-base alloy for deposition by plasma transferred arc[13], for example.

The aging temperature has also a significant influence on the hardness since the latter is lowered when aging was realized at a higher temperature. This can be due to the small decrease in carbide fraction, but the little morphological change of the carbides (which become more compact and/or fractioned) induced by the aging treatment can also be

responsible of this decrease in hardness. Such an effect was already encountered for cobalt–base superalloys in which long exposures to high temperature induced fragmentation of their interdendritic tantalum carbides, and then to a decrease in room temperature hardness[14].

The hardness linearly increases with the volume fraction of carbides, which suggests that the hardness of the whole alloy may be a linear combination of the volume fractions of the two phases, with the separated hardness of matrix and carbides as multiplying factors. To examine this possibility, which could be of a great interest for prediction of hardness from carbides fractions (which can be given by Thermo-Calc calculations), it was attempted to fit the curve of the measured hardness with several laws, all of the type:

$$Hv\ (all) = (1 - f_{vol}(carb)) \times Hv(mat) + f_{vol}(carb) \times Hv\ (carb)$$

with :

* **Hv (all)** = average Vickers hardness of the whole alloy (load: 30kg)
* **f_{vol}(carb)** = average value of surface fraction measured by microanalysis
* **Hv(carb) =** 1192 (value obtained for the very coarse carbide found in the Ni20 aged at 1,000°C, obtained by micro-hardness measurement with a 32g load)
* **Hv(mat)** = average value of the hardness (load 30kg) of the binary alloy Ni-30Cr (curves designed in Fig. 5 by "**theo1**")

  or Hv(mat) = average value of the micro-hardness (load 8g) of the Ni-30Cr (curves designed in Fig. 5 by "**theo2**")

  or Hv(mat) =average value of the five micro-hardness (load 8g) values obtained in the matrix of the considered alloy for the considered aging temperature (curves designed in Fig. 5 by "**theo3**").

The three types of theoretic curves were superposed with the experimental macro-hardness one in Fig. 5, in which each of the three graphs corresponds to a given aging temperature. It appears that the first theoretic curve ("theo1", with calculation from the Hv30kg average value of the Ni-30wt.%Cr alloy) is closer to the real curve than the two other theoretic curves. However, the fit is very good only for the alloys with the lowest carbon contents. The difference is significantly greater for the Ni12 to Ni20 alloys. It can be noticed that the latter are precisely the ones in which the dendrite structure of matrix is the less present or even inexistent (e.g. Ni20). But this is probably not the main reason of the enhanced deviation of real hardness form the law of mixture.

Another possible explanation can be summarized as follows. During the hardness test, only the matrix of the alloy is deformed when indentation begins, since carbides are too hard and are only displaced by the movement of the local matrix being plastically deformed. At the end of indentation carbides probably act more, since they are closer to each other, and the matrix, hardened by its plastic deformation, is simultaneously more resistant against additional deformation. When the carbon content is higher, then the volume fraction of carbides higher, the hardening of matrix during indentation is achieved sooner since a smaller volume of matrix is plastically deformed for a same load applied (because of the lower volume fraction of matrix in the alloy). This, added to the sooner increase in neighborhood of the more present carbides, leads to an increase in hardness which is found both by models and in reality. However, real hardness does not increase as quickly as a law of mixture since the carbides are not deformed, neither in the low carbon alloys, nor in the high carbon alloys (or very few deformed in the later ones), since the difference of hardness between matrix and carbides is too great in these nickel alloys. Notably, for especially high carbides volume fractions, the real hardness almost stops increasing when the carbon content increases above 1.2 wt.%, although the laws of mixtures mathematically go on giving higher values of calculated hardness. This may be different for chromium carbides–containing alloys displaying a matrix harder than the nickel-chromium one of the alloys studied here.

5. Conclusion

The ternary Ni-30Cr-xC alloys, which are the bases of several Ni-based superalloys (and which are themselves suitable for high temperature applications because of their high refractoriness[15] and their good behaviour in oxidation by hot air[16]), are probably not especially difficult to machine, even if carbides are very present in some of them. Indeed, the hardness, which effectively increases with carbon from the binary Ni30Cr alloy (about 120 Hv_{30kg}), does not reach very high values (maximum of about 270 Hv_{30kg} with near 27 vol.% of carbides). Moreover an aging treatment can reduce this hardness (e.g. 50 Hv_{30kg} less). Unfortunately there is seemingly no simple relationship between macro-hardness, the carbide fraction and the separated hardness of the two phases present. A first reason should be the loss of the primary dendrites when carbon begins to be too present. More probably, the laws of mixtures cannot be used because of the too large difference of hardness between the two phases present in the alloys, which gives a too predominant role to matrix in the plastic

deformation, notably at the beginning of indentation. This study will be continued in a second article[17], concerning chromium–containing cobalt–base alloys.

Acknowledgments

The author gratefully thanks Pierric LEMOINE who elaborated and heat-treated some of the studied alloys.

References

[1] M.A. Engelman and C. Blechner: *The New York Journal of Dentistry*, 1976, **46**, 232-235.

[2] E.F. Huget, N. Dvivedi, H.E. Cosner*: The Journal of the American Dental Association*, 1977, **94**, 87-90.

[3] E.F. Bradley: 'Superalloys: A technical guide'; 1988, Metals Park, ASM International.

[4] C.T. Sims and W.C. Hagel: 'The superalloys'; 1972, New York, John Wiley & Sons.

[5] A. Klimpel, L.A. Dobrzanski, A. Lisiecki and D. Janicki: *J. Mater. Process. Tech.*, 2005, **164-165**, 1068-1073.

[6] Z.T. Wang and H.H. Chen: *Mocaxue Xuebao Tribology*, 2005, **25**, 203-206.

[7] H. Han, S. Baba, H. Kitagawa, S. A. Suilik, K. Hasezaki, T. Kato, K. Arakawa and Y. Noda: *Vacuum*, 2005, **78**, 27-32.

[8] D. Zhang and X. Zhang: *Surf. Coat. Tech.*, 2005, **190**, 212-217.

[9] Thermo-Calc version N: "Foundation for Computational Thermodynamics" Stockholm, Sweden, Copyright (1993, 2000).

[10] A. Dinsdale and T. Chart: MTDS NPL, unpublished work, 1986.

[11] A. Gabriel, C. Chatillon and I. Ansara: *High Temperature Science*, 1988, **25**, 17-54.

[12] J. O. Andersson: *Calphad*, 1987, **11**, 271-276.

[13] K. Gurumoorthy, M. Kamaraj, K. P. Rao, A. S. Rao and S. Venugopal: *Mat. Sci. Eng. A*, 2007, **456**, 11-19.

[14] S. Michon, L. Aranda, P. Berthod and P. Steinmetz: *Rev. Met. –C.I.T./Sci. Gen. Mater.*, 2004, **9**, 651-662.

[15] P. Berthod, P. Lemoine, and L. Aranda: *submitted to Calphad.*

[16] P. Berthod, P. Lemoine, and L. Aranda: *Mater. Sci. Forum*, to be published.

[17] P. Berthod: submitted to *Mater. Sci. Technol.*

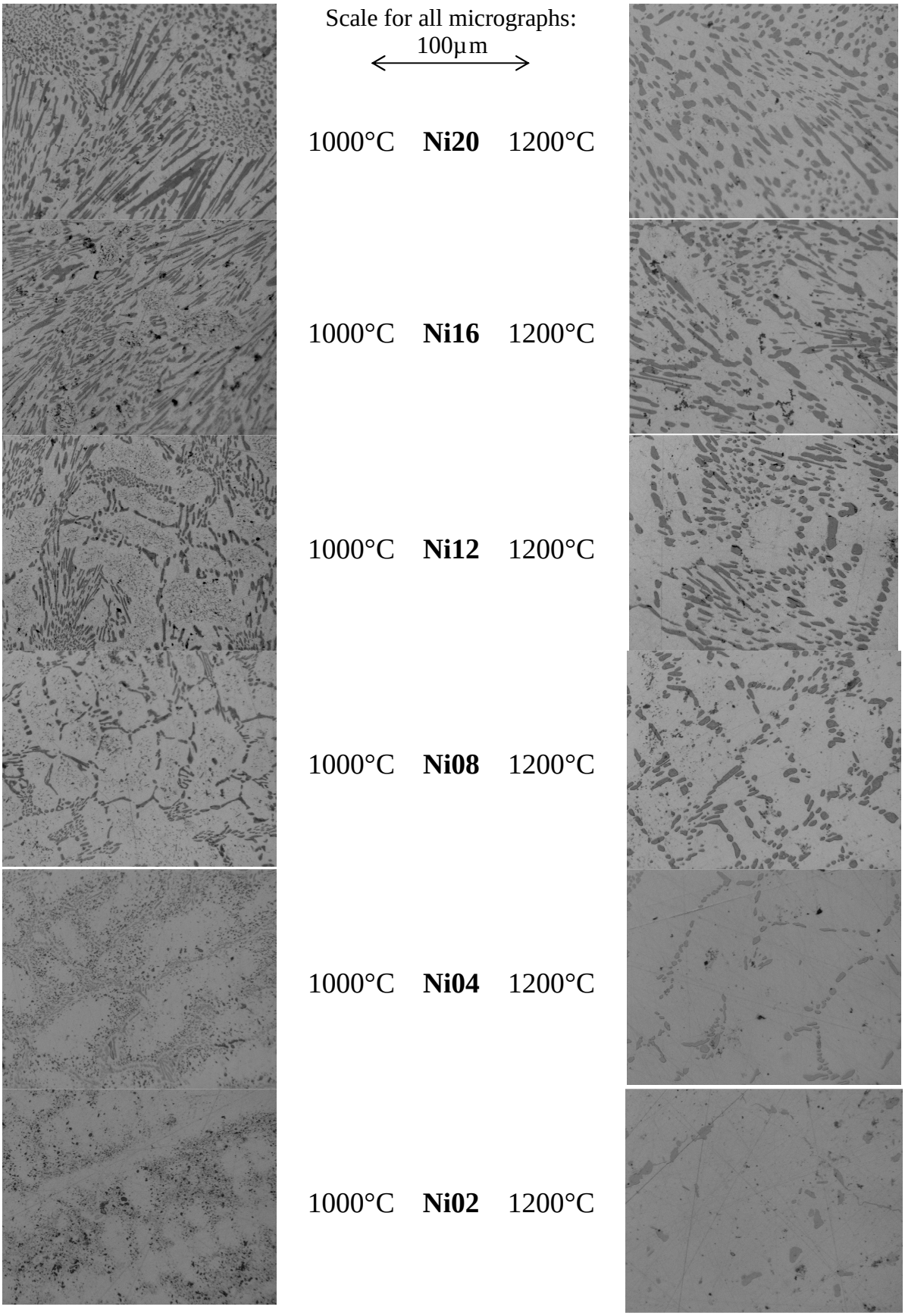

Fig. 1 Microstructures of the six Ni-based C-containing alloys after 50 hours spent at the two extreme temperatures

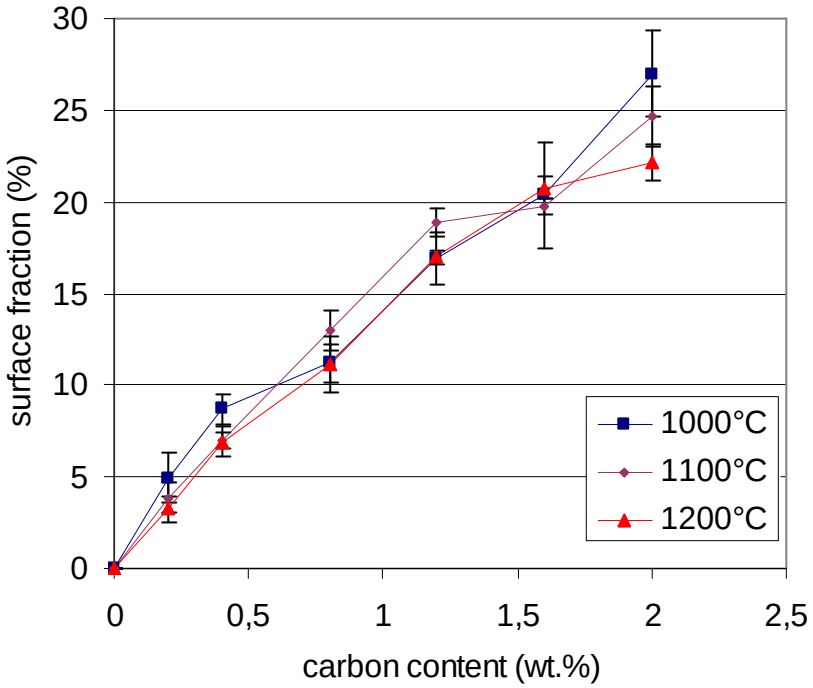

Fig. 2 Surface fractions of all alloys plotted versus their carbon content for the three aging temperatures; determination by image analysis on three optical micrographs after Groesbeck etching (average value ± standard deviation)

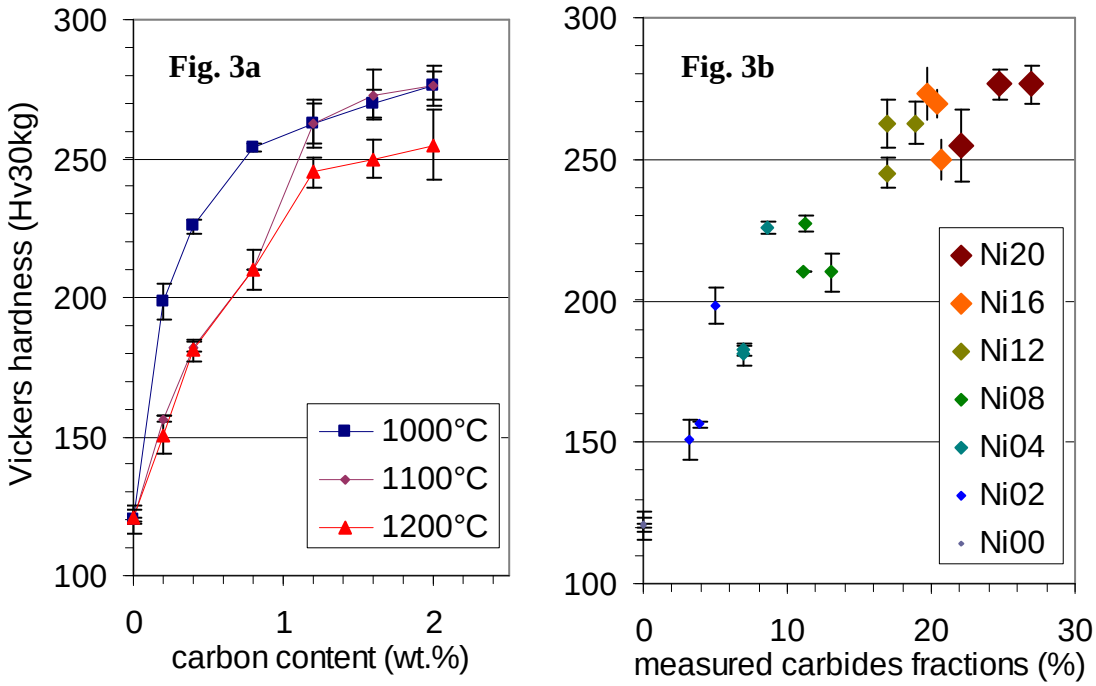

Fig. 3 Vickers hardness (30kg) of all alloys plotted versus their carbon content (Fig. 3a, left hand side) and versus their carbide fractions (Fig. 3b, right hand side) for the three aging temperatures (average value ± standard deviation)

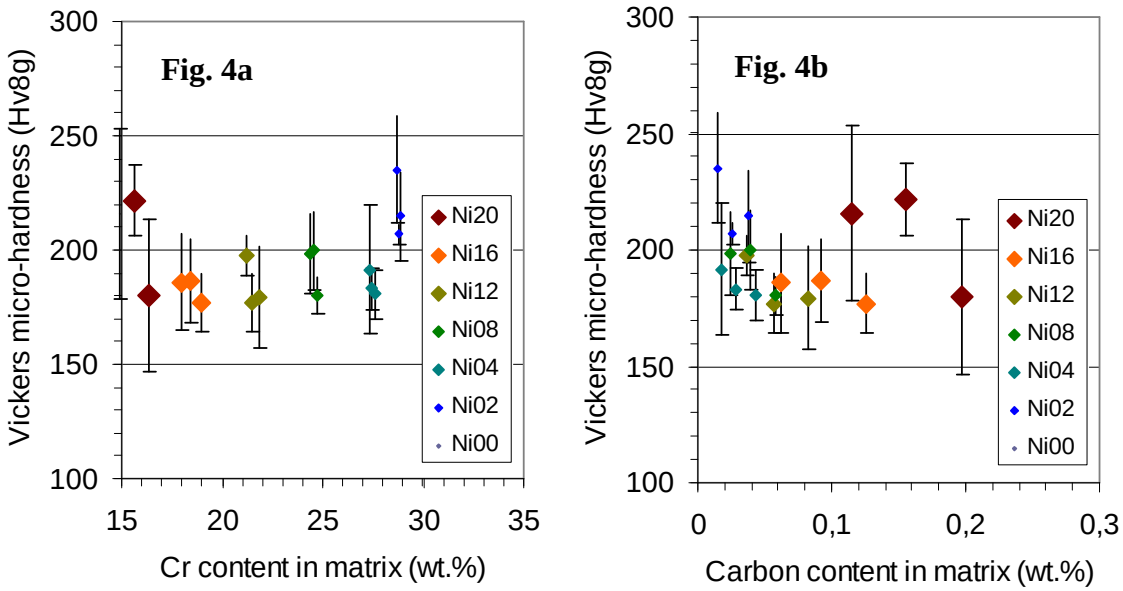

Fig. 4 Vickers micro-hardness (8 g) of all alloys'matrix plotted versus their chromium content (Fig. 4a, left hand side) and versus their carbon content (Fig. 4b, right hand side) for the three aging temperatures (average value ± standard deviation)

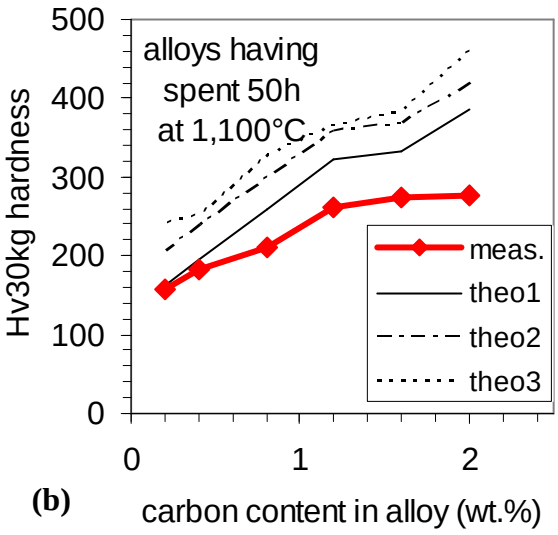

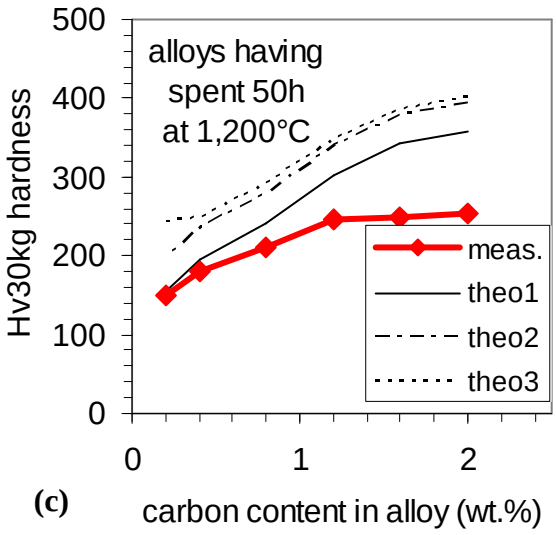

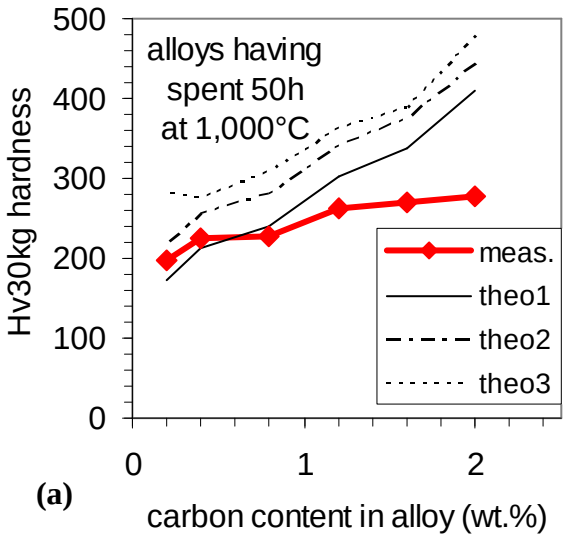

Fig. 5

Comparison of the measured hardness of all alloys for 1000°C **(a)**, 1,100°C **(b)** and 1,200°C **(c)** with the three types of theoretic hardness calculated from the hardness of matrix and the hardness of carbides